

# The COMAP 30 GHz Galactic Plane Survey

(Dated: December 1, 2025)

## I. INTRODUCTION

This report aims to use data obtained by the CO Mapping Array Project (COMAP) of the region surrounding M31 to quantify various features of the different feeds and attempt to find improvements in the way individual feed maps are combined.

The COMAP survey covers frequencies between 26 and 34 GHz, with more detailed specifications of the telescope and maps created shown in Table I

**TABLE I:** Specifications of the COMAP telescope at the Owens Valley Radio Observatory and the maps created.(Lamb et al. 2022).

Dish diameter	10.4 m
Angular resolution	4.5'
Number of feeds	19
Frequency range	26 - 34 GHz
Number of bands	8
Integration time	20 ms
Calibration Accuracy	$3.2\% \pm 0.1\%$
Coverage <sup>a</sup>	$118^\circ \lesssim l \lesssim 124^\circ$ $-23^\circ \lesssim b \lesssim -20^\circ$
Pixel Size	1'
Map Units	K

<sup>a</sup> Galactic coordinates covered in the maps of M31

## II. INDIVIDUAL FEED MAPS

### A. Source Analysis

Nearby M31 a bright source can be seen at around 30 GHz. This is the source 5C 3.50 with information on the source being obtained from the SIMBAD catalogue<sup>1</sup>. On each of the individual feed maps, a 2D circular Gaussian was fitted to the source to determine the flux density and the position of the centre of the source.

The SIMBAD catalogue<sup>1</sup> gives the expected position of 5C 3.50 as  $l = 120.322^\circ$ ,  $b = -21.187^\circ$ . By comparing this value to the positions taken from the Gaussian fits for each map; an offset of  $1.17 \pm 0.03$  arcminutes is found from taking the average shift. Fig 1 shows the relative positions of the source on the maps against the expected

location found by rotating the sphere all the points lie on so that the source is at  $l = 0^\circ$ ,  $b = 0^\circ$ .

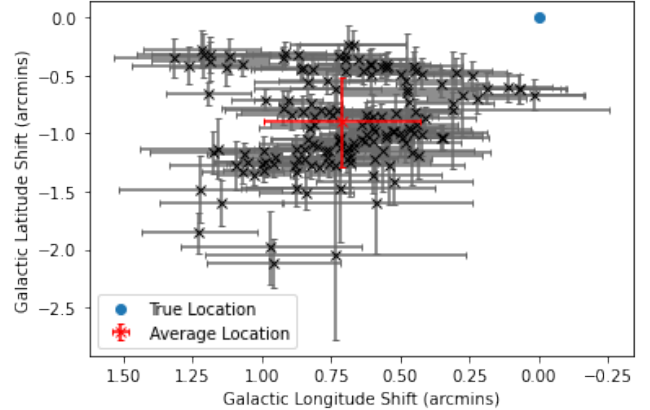


**FIG. 1:** Measured central position of the source 5C 3.50 from every map along with an averaged position and the true source position taken from the SIMBAD catalogue, with all points rotated so the true source position lies at  $l = 0^\circ$ ,  $b = 0^\circ$

From these fits the flux density of the source can also be calculated using:

$$F = 2\pi\sigma^2 A, \quad (1)$$

where  $\sigma$  is the standard deviation and  $A$  is the amplitude of the Gaussian fit. Fig 2 shows the values of the flux densities measured for each of the feeds. The feeds appear

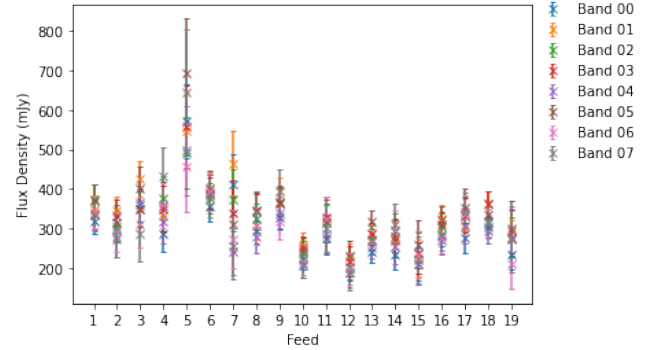


**FIG. 2:** Measured flux densities of the source 5C 3.50 from each of the feeds

to be consistent with each other, but feed 5 clearly has extremely large errors with a much higher value of the measured flux compared to other feeds. This is likely due to issues when fitting a source with a low signal-to-noise ratio. An example of this is shown in Fig 3, where 5C 3.50 is less distinct from the background in the Band 00 Feed 05 data, than the Band 00 Feed 01 data. All values

<sup>1</sup> SIMBAD data on 5C 3.50 can be found at: <https://simbad.u-strasbg.fr/simbad/sim-id?Ident=5C+3.50>, accessed December 1, 2025

for the measured flux densities and signal-to-noise values can be found in Appendix A.

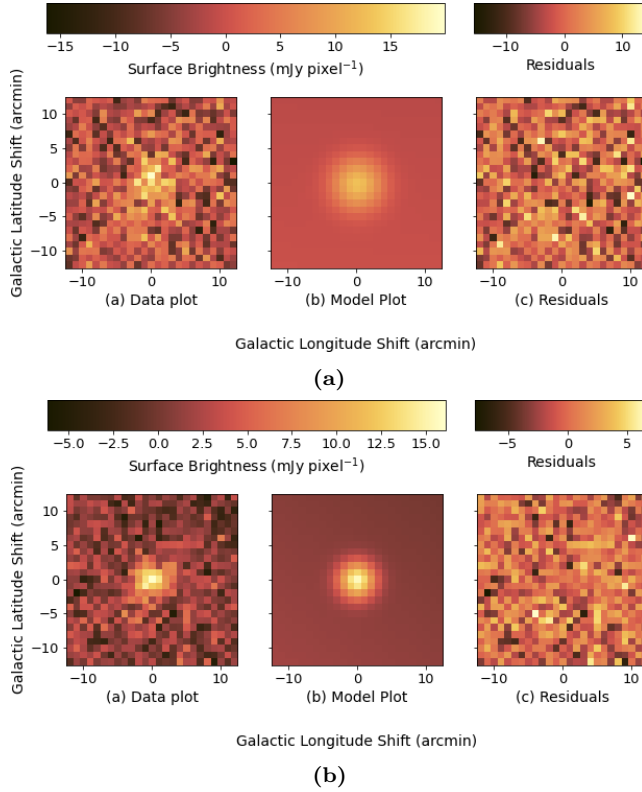


**FIG. 3:** Gaussian fits for the source 5C 3.50 from the (a) Band 00 Feed 05 map, (b) Band 00 Feed 01 map.

A final value for the flux density of the source in each band is found by calculating the weighted average across the feeds using the uncertainties in each measurement to find the weights, shown in Table II.

## B. Noise Levels

The next area I investigated was the noise levels of each of the maps by looking at the red noise and white noise levels of each map. This was performed by first taking a 2D Fourier transform of the centre of the maps from  $l = 119^\circ 49'$ ,  $b = -20^\circ 54'$  to  $l = 122^\circ 57'$ ,  $b = -22^\circ 14'$ . This area was chosen because visually it appeared to be the largest area that did not overlap with any of the extremely noisy edges of the maps.

Then each data point in the 2D power spectrum was given a radial frequency value  $k_r$  by calculating:

$$k_r = \sqrt{k_x^2 + k_y^2}, \quad (2)$$

where  $k_x$  and  $k_y$  are the frequencies in the x and y directions, respectively. By binning the 2D power spectrum into 100 bins with respect to the radial frequency value and taking the average value of the power within each bin, the 2D power spectrum can be collapsed to a 1D

power spectrum. An example of the 2D and 1D power spectrums created can be seen in Fig 4

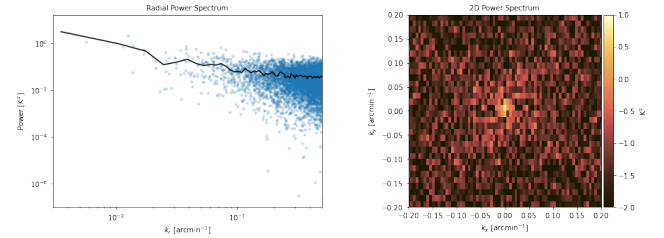


**FIG. 4:** Power spectrums created using the map from band 00 feed 03. The 2D power spectrum (right) shows a faint cross in the data which matches observations of systematic effects in the map. The 1D power spectrum (left) shows the individual power values (blue dots) and the averaged value in each bin (black line)

The binned 1D power spectrum was then fitted using:

$$P = \sigma_R^2 \left( \frac{\nu_{\text{knee}}}{k_r} \right)^\alpha + \sigma_W^2, \quad (3)$$

where  $\sigma_R$  is the red noise,  $\sigma_W$  is the white noise,  $\alpha$  is the spectral index and  $\nu_{\text{knee}}$  is the knee frequency set to 0.1 arcmin<sup>-1</sup>. An example of a fitted power spectrum can be seen in Fig 5

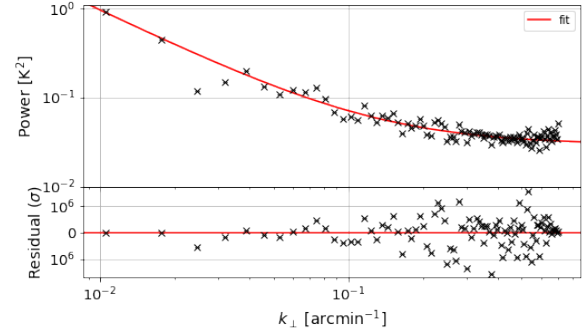


**FIG. 5:** Fitted 1D power spectrum created using the map from band 00 feed 03

The values of these fits for band 00 can be seen in Table III.

Separately from the noise levels of each map, some of the feeds have strong systematic effects that can be seen in the maps<sup>2</sup>. These systematics are from various sources in the different feeds; for example, feed 03 shows extra 1/f noise from the scans that hasn't been removed during

<sup>2</sup> All the initial maps can be found in the Initial Maps file.

**TABLE II:** Band averaged flux density of 5C 3.50 calculated using the weighted average of the measured flux density of all 19 feeds.

Band 00	Band 01	Band 02	Band 03	Band 04	Band 05	Band 06	Band 07
280±20	321±19	308±15	316±16	277±17	320±20	289±15	290±20

**TABLE III:** Values of fits for each feed from band 00 using Eqn 3

Feed	$\sigma_W (\times 10^{-1})$	$\alpha$	$\sigma_R (\times 10^{-1})$
Feed 01	1.28±0.03	1.53±0.17	1.73±0.07
Feed 02	1.39±0.03	1.6±0.22	1.55±0.08
Feed 03	1.72±0.06	1.35±0.24	2.05±0.11
Feed 04	2.08±0.03	1.82±0.36	1.59±0.16
Feed 05	2.78±0.15	1.12±0.22	3.52±0.16
Feed 06	1.55±0.06	1.23±0.22	1.83±0.09
Feed 07	3.39±0.06	1.49±0.38	2.25±0.24
Feed 08	1.25±0.02	1.62±0.24	1.3±0.07
Feed 09	1.21±0.02	2.02±0.21	1.63±0.09
Feed 10	1.13±0.01	1.96±0.29	0.97±0.07
Feed 11	1.63±0.07	1.27±0.21	2.1±0.1
Feed 12	1.79±0.04	1.59±0.22	1.93±0.1
Feed 13	1.28±0.04	1.37±0.22	1.57±0.08
Feed 14	2.08±0.04	1.69±0.33	1.88±0.16
Feed 15	1.98±0.26	0.85±0.24	2.95±0.15
Feed 16	1.23±0.04	1.44±0.26	1.36±0.08
Feed 17	1.81±0.05	1.3±0.24	1.87±0.1
Feed 18	1.01±0.02	1.98±0.27	1.16±0.08
Feed 19	1.75±0.03	1.52±0.32	1.34±0.11

processing. Another example is shown in Feed 09 where large structures can be seen, which are caused by residual atmosphere and ground signals. Finally, the systematics seen in Feed 16 are most likely caused by steps in the scans, where the atmosphere effects are not averaging down correctly. An example of all these maps can be seen in Fig 6.

### C. Simulated Noise Maps

Using the RMS layers provided alongside the individual maps, simulated noise maps were created by multiplying the RMS layers by an array of random numbers from a normal distribution. Fig 7 shows an example of an RMS layer and the simulated map it produces.

Each of these simulated noise maps was then used to repeat the process described in the previous section. Fourier transforming the centre of the map and then binning the 2D power spectrum produced using the radial frequency to create a 1D power spectrum. However, when fitting these spectrums there is no red noise component, so only the white noise value was in the fit.

The white noise levels of the simulated maps were then

compared to the values of red and white noise in the real maps to see how well the RMS layers matched up to the true errors in the map. The full tables of these ratios can be found in Appendix B. As can be seen from Table VIII, the majority of the white noise ratios are within 2 standard deviation of one. In cases where the ratio is above one by more than 2 standard deviations it appears to follow across the entire feed, for example feed 04. This suggests that in certain feeds the error is being underestimated when creating the RMS layer.

## III. COMBINED MAPS

### A. No Additional Weighting

To create an improved map with lower noise levels the individual feed maps are combined to produce a map with more data and so a lower noise level. An estimate can be obtained for the expected red and white noise level if the maps are optimally combined by assuming that both reduce as Gaussian noise. This is done by calculating the average noise level of the maps and dividing it by the square root of the number of maps combined. Here, I am working with the band 00 data with the optimal values shown in Table IV

**TABLE IV:** Expected values for red and white noise from an optimally combined map

$\sigma_W (\times 10^{-2})$	$\sigma_R (\times 10^{-2})$
2.71±0.17	4.1±0.2

An initial map is created by using the given RMS layers, see Fig 7, to weight each pixel of the individual maps in the combination. The final map created is shown in Fig 8

Repeating the method used on the individual maps to estimate the white and red noise gives the values in Table V. The power spectrum for the combined map, shown in Fig 8, clearly has two different slopes in the red noise dominated scales. At larger scales it is significantly shallower compared to the fitted values, which suggests the combination may have done better at removing the red noise at larger scales.

Comparing these to the optimal values in Table IV, we can see that neither the white noise or the red noise have been reduced to the levels we expect for an optimally combined map. However, the white noise has been reduced significantly more than the red noise, which was expected because the red noise has 1/f properties, so it

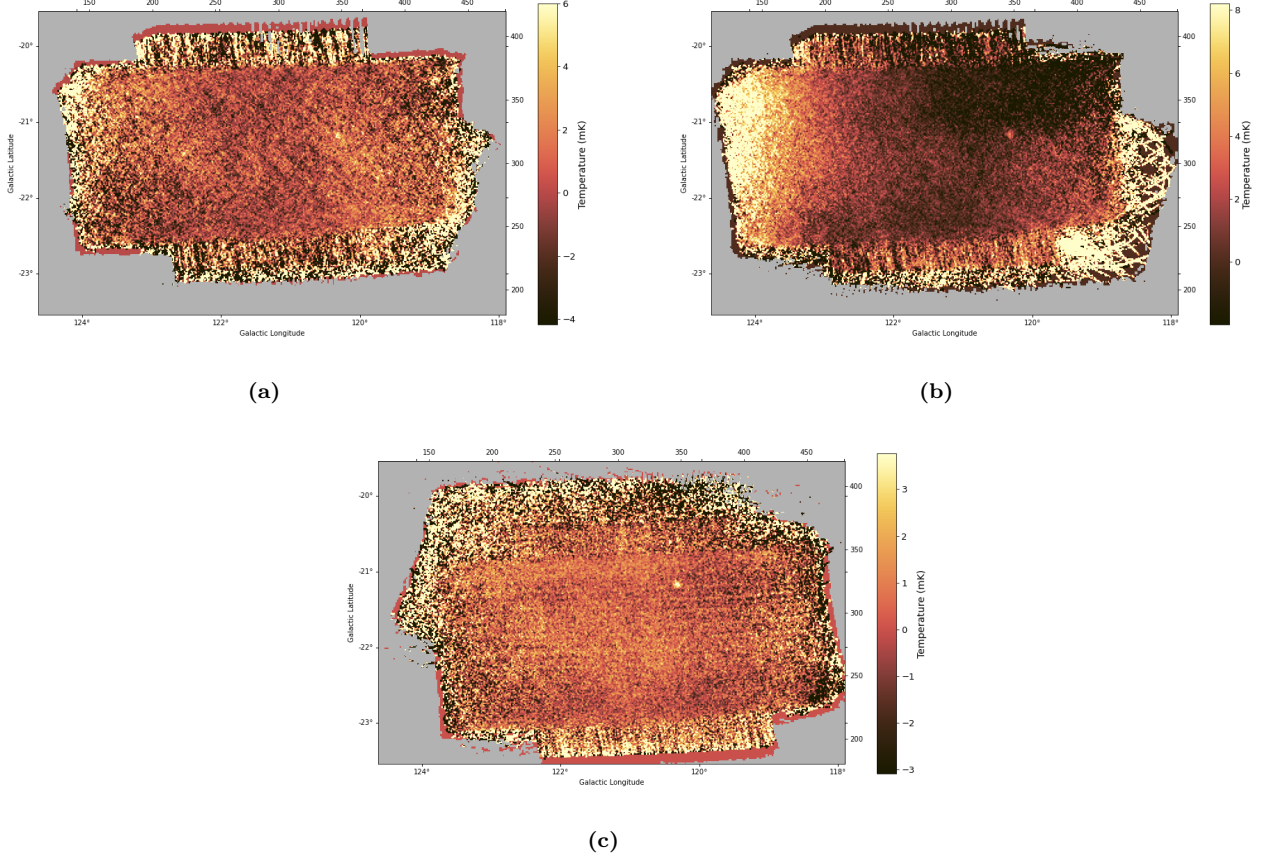


**FIG. 6:** (a) Map from band 07 feed 03 showing extra 1/f noise in the scans. (b) Map from band 07 feed 09 showing residual ground and atmosphere signal. (c) Map from band 07 feed 16 showing steps in the scans caused to atmosphere effects not averaging down correctly.

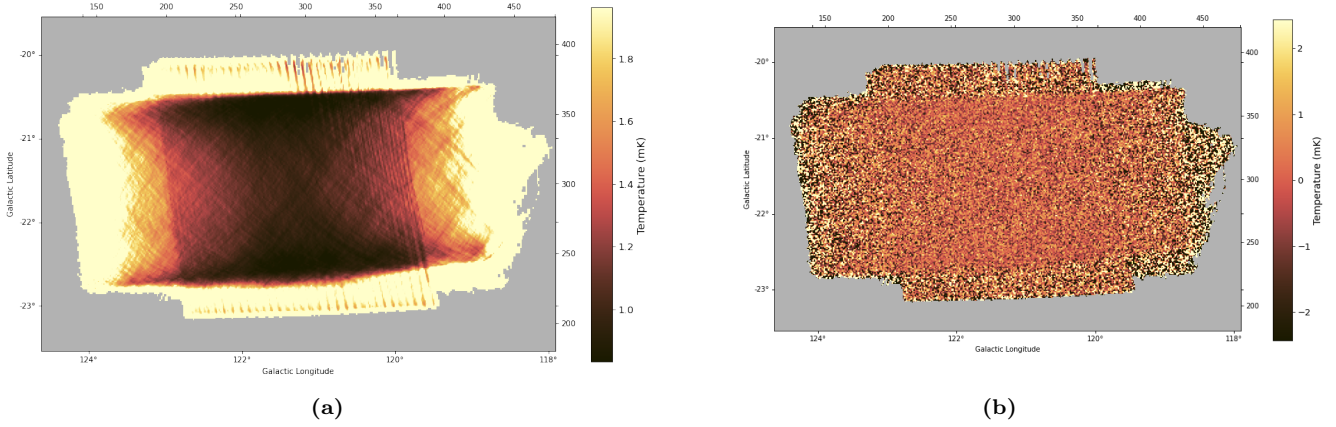


**FIG. 7:** (a) shows the RMS layer from Band 00 Feed 02 and (b) shows the simulated map created using this RMS layer

is unlikely to be reduced as perfect Gaussian noise. This does suggest that there are potentially improvements we can make to the way the maps are combined.

## B. Noise Ratio Weighting

In an attempt to improve the map further each of the RMS maps was multiplied by the ratio between the white noise level of the real and simulated maps, with the values

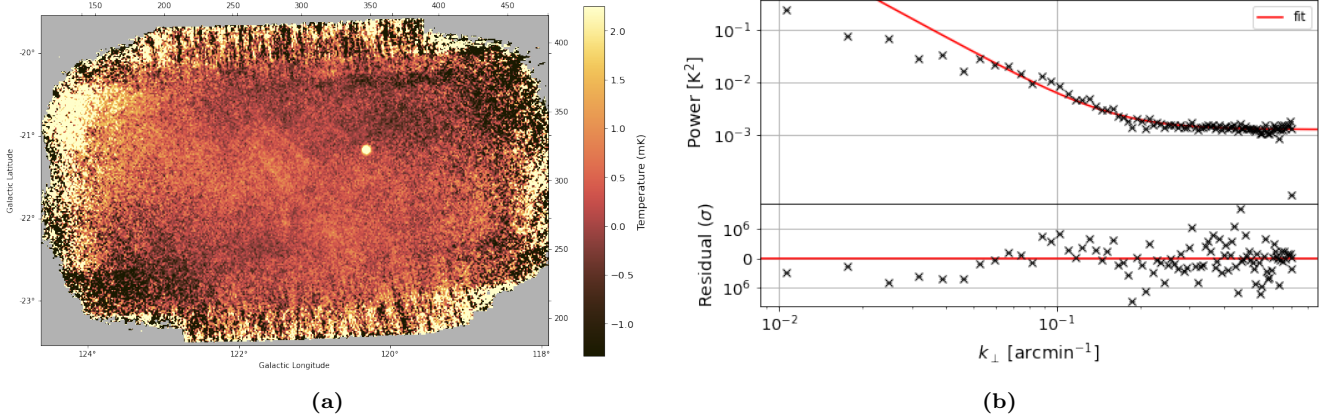


**FIG. 8:** (a) Map created when combining all of the 19 feeds for band 00 using just the RMS layer to weight each pixel. (b) 1D power spectrum from the map in (a)

used shown in Table VIII. This will reduce the weighting of pixels where the measured white noise of the map is larger than the RMS layer seems to suggest. However, due to how close all the ratios are to 1, this has had no visual effect on the map and the changes to the fitted values in the power spectrum are much less than  $1\sigma$ .

Another attempt was made by multiplying the RMS layer by the ratio between the red noise level of the real map and the white noise level of the simulated maps, with the values shown in Table IX. This was an attempt to more optimally weight the maps with respect to the red noise and bring the combined maps red noise level lower. However, in the final map the red noise has been reduced by less than  $1\sigma$ , whilst the white noise has increased by  $\sim 5\sigma$ .

The values for the power spectrum fits in this section can be found in Table V

**TABLE V:** Fitted results for each of the combined maps

Map	$\sigma_W (\times 10^{-2})$	$\alpha$	$\sigma_R (\times 10^{-2})$
No Weighting	$3.56 \pm 0.04$	$2.90 \pm 0.17$	$7.1 \pm 0.3$
White Noise Ratio	$3.57 \pm 0.04$	$2.90 \pm 0.17$	$7.1 \pm 0.3$
Red Noise Ratio	$3.77 \pm 0.04$	$2.89 \pm 0.18$	$7.0 \pm 0.3$

#### IV. CONCLUSION

In conclusion we have shown that the RMS layers appear to closely match the white noise levels of the real maps for most of the feeds and bands with in the worst case the white noise level is only  $\sim 20\%$  higher than predicted by the simulated maps.

We also see that the measured flux density appears to be mostly consistent across the feeds and bands with a final result for the flux density of  $\sim 300$  mJy, with every band average flux density within  $1.5\sigma$  of this value.

Finally, after attempting to weight the maps in slightly different ways using the white and red noise, we conclude that currently using the RMS maps alone to weight the maps is the optimal method to get the lowest noise levels. However, by comparing the current noise levels, to the expected optimal noise levels found by assuming Gaussian noise, we see that there is potentially still some room for improvement.

### Appendix A: Flux Measurements

Table VI shows the flux density measurements obtained from the 5C 3.50 source on all the individual feed maps using Gaussian fits and Table VII shows the signal-to-noise for each of these fits.

**TABLE VI:** Measured flux density of the source 5C 3.50 for all bands and feeds in mJy.

	Band 00	Band 01	Band 02	Band 03	Band 04	Band 05	Band 06	Band 07
Feed 1	330±41	362±47	390±48	353±47	372±59	393±57	357±56	355±59
Feed 2	309±42	352±43	310±49	336±50	274±54	315±56	298±64	279±60
Feed 3	361±52	433±56	357±60	362±62	389±78	420±75	317±77	347±150
Feed 4	302±53	349±57	397±65	367±68	334±66	364±71	369±74	424±92
Feed 5	685±148	670±150	646±164	712±194	606±175	865±231	640±188	749±221
Feed 6	354±44	404±49	378±46	388±51	389±56	402±59	397±59	387±67
Feed 7	459±103	472±113	508±129	412±130	271±78	340±104	301±97	270±100
Feed 8	296±37	309±43	329±44	348±50	285±49	345±54	317±57	352±65
Feed 9	334±38	402±45	370±46	379±49	343±54	368±57	325±57	420±90
Feed 10	226±30	263±33	248±35	258±36	208±35	254±37	224±41	212±39
Feed 11	277±54	327±61	313±61	266±57	283±65	316±74	317±79	290±82
Feed 12	198±40	231±43	207±41	220±47	203±48	236±50	219±53	124±34
Feed 13	239±32	284±32	273±34	286±33	252±33	315±36	263±37	268±42
Feed 14	242±48	274±53	298±54	227±40	255±49	276±53	300±56	312±59
Feed 15	202±52	222±65	227±63	224±60	207±60	248±74	220±67	214±67
Feed 16	282±31	326±40	306±37	312±38	271±41	324±41	280±43	290±45
Feed 17	287±44	311±50	341±51	336±52	307±50	354±56	335±58	344±56
Feed 18	304±31	365±34	321±33	369±38	296±37	337±39	319±42	323±48
Feed 19	232±48	270±57	269±69	280±77	361±131	412±124	377±149	359±126

**TABLE VII:** Signal-to-noise ratio obtained from each individual feed map when fitting the source 5C 3.50

	Band 00	Band 01	Band 02	Band 03	Band 04	Band 05	Band 06	Band 07
Feed 1	8.01	7.62	8.11	7.45	6.29	6.87	6.42	6.01
Feed 2	7.29	8.25	6.28	6.73	5.12	5.63	4.66	4.69
Feed 3	6.88	7.79	5.94	5.85	4.97	5.63	4.13	2.31
Feed 4	5.7	6.14	6.13	5.42	5.04	5.14	4.96	4.62
Feed 5	4.63	4.46	3.93	3.66	3.47	3.74	3.41	3.39
Feed 6	8.14	8.23	8.2	7.64	7.0	6.79	6.72	5.75
Feed 7	4.45	4.17	3.93	3.17	3.5	3.26	3.09	2.71
Feed 8	8.07	7.18	7.49	6.99	5.85	6.35	5.54	5.46
Feed 9	8.73	8.9	8.08	7.67	6.35	6.42	5.69	4.69
Feed 10	7.52	7.86	7.12	7.21	5.94	6.82	5.52	5.42
Feed 11	5.16	5.32	5.13	4.67	4.34	4.27	4.0	3.56
Feed 12	4.97	5.33	5.02	4.72	4.18	4.7	4.15	3.69
Feed 13	7.47	8.94	8.0	8.66	7.68	8.85	7.08	6.31
Feed 14	5.03	5.16	5.49	5.7	5.18	5.2	5.37	5.29
Feed 15	3.88	3.4	3.59	3.73	3.44	3.37	3.3	3.17
Feed 16	9.11	8.14	8.2	8.29	6.66	7.85	6.47	6.42
Feed 17	6.58	6.26	6.64	6.52	6.13	6.28	5.81	6.11
Feed 18	9.91	10.58	9.76	9.63	8.02	8.76	7.6	6.77
Feed 19	4.84	4.78	3.93	3.63	2.76	3.33	2.52	2.85

## Appendix B: Simulated Map Ratios

From fitting the 1D power spectrums of both the real and simulated maps the ratios between the white noise of both maps are shown in Table VIII and the ratios between the red noise of the real maps and the white noise of the simulated maps is shown in Table IX.

**TABLE VIII:** Ratio of white noise between real maps and simulated maps

	Band 00	Band 01	Band 02	Band 03	Band 04	Band 05	Band 06	Band 07
Feed 1	1.07±0.03	1.01±0.03	1.07±0.04	1.04±0.04	1.02±0.06	1.08±0.04	1.08±0.05	1.05±0.06
Feed 2	1.04±0.02	1.04±0.02	1.04±0.03	1.06±0.02	1.07±0.03	1.05±0.03	1.07±0.03	1.09±0.04
Feed 3	1.00±0.04	1.02±0.03	1.02±0.03	1.03±0.02	1.00±0.04	1.02±0.03	1.01±0.04	1.03±0.05
Feed 4	1.07±0.02	1.08±0.02	1.11±0.02	1.11±0.04	1.14±0.04	1.17±0.03	1.14±0.04	1.11±0.04
Feed 5	1.05±0.06	1.05±0.04	1.04±0.06	1.02±0.06	1.04±0.05	1.03±0.05	0.99±0.07	1.02±0.05
Feed 6	0.97±0.04	0.99±0.03	0.99±0.03	0.99±0.03	1.0±0.04	1.02±0.03	1.01±0.04	1.01±0.04
Feed 7	1.02±0.02	1.01±0.02	1.04±0.02	1.04±0.02	1.04±0.02	1.03±0.02	1.04±0.02	1.05±0.02
Feed 8	1.02±0.02	1.0±0.03	1.0±0.04	0.88±0.09	0.91±0.08	0.87±0.1	0.88±0.1	0.81±0.14
Feed 9	1.05±0.02	1.06±0.01	1.06±0.02	1.06±0.02	1.07±0.02	1.07±0.02	1.09±0.02	1.1±0.02
Feed 10	1.03±0.01	1.03±0.01	1.05±0.01	1.03±0.02	1.04±0.02	1.05±0.02	1.06±0.01	1.06±0.02
Feed 11	1.0±0.04	0.98±0.05	1.01±0.04	0.99±0.04	1.02±0.04	1.02±0.04	1.03±0.04	1.04±0.04
Feed 12	1.07±0.02	1.05±0.02	1.08±0.03	1.08±0.02	1.08±0.03	1.09±0.03	1.09±0.03	1.09±0.04
Feed 13	1.04±0.04	1.02±0.02	1.04±0.04	1.01±0.03	1.01±0.04	1.03±0.03	1.02±0.04	1.05±0.03
Feed 14	1.07±0.02	1.07±0.02	1.08±0.02	1.08±0.02	1.09±0.02	1.09±0.02	1.07±0.03	1.09±0.02
Feed 15	0.89±0.12	0.93±0.08	0.95±0.11	0.89±0.15	0.91±0.14	0.87±0.18	0.95±0.11	0.93±0.12
Feed 16	0.98±0.03	0.88±0.08	0.97±0.04	0.96±0.05	0.9±0.08	0.96±0.05	0.89±0.09	0.91±0.07
Feed 17	1.07±0.03	1.05±0.04	1.04±0.04	1.03±0.05	1.04±0.04	1.03±0.03	1.05±0.04	1.08±0.03
Feed 18	1.03±0.02	1.02±0.01	1.04±0.02	1.05±0.02	1.06±0.02	1.06±0.02	1.07±0.02	1.04±0.03
Feed 19	1.04±0.02	1.04±0.02	1.02±0.04	1.05±0.03	1.07±0.04	1.01±0.06	1.06±0.04	1.06±0.05

**TABLE IX:** Ratio of red noise from real maps and white noise from simulated maps

	Band 00	Band 01	Band 02	Band 03	Band 04	Band 05	Band 06	Band 07
Feed 1	1.44±0.06	1.27±0.06	1.6±0.07	1.47±0.05	1.75±0.06	1.69±0.06	1.73±0.07	1.88±0.07
Feed 2	1.16±0.06	1.14±0.06	1.28±0.07	1.21±0.07	1.31±0.06	1.28±0.07	1.4±0.06	1.45±0.07
Feed 3	1.2±0.06	1.01±0.07	1.08±0.06	1.01±0.06	1.23±0.06	1.05±0.07	1.29±0.06	1.46±0.07
Feed 4	0.81±0.08	0.82±0.08	0.92±0.07	1.11±0.09	1.21±0.08	1.1±0.07	1.24±0.07	1.32±0.06
Feed 5	1.32±0.06	1.12±0.06	1.3±0.06	1.26±0.06	1.22±0.06	1.23±0.06	1.23±0.06	1.3±0.06
Feed 6	1.15±0.05	1.01±0.05	1.16±0.05	1.18±0.05	1.23±0.06	1.2±0.06	1.34±0.06	1.48±0.06
Feed 7	0.68±0.07	0.65±0.07	0.7±0.06	0.71±0.07	0.82±0.06	0.77±0.06	0.89±0.06	0.96±0.06
Feed 8	1.06±0.06	1.1±0.05	1.29±0.06	1.52±0.05	1.49±0.05	1.52±0.05	1.54±0.06	1.62±0.06
Feed 9	1.42±0.08	1.59±0.07	1.53±0.08	1.27±0.07	1.28±0.07	1.3±0.07	1.25±0.08	1.35±0.07
Feed 10	0.89±0.07	0.94±0.07	0.92±0.08	0.98±0.07	0.99±0.07	0.95±0.08	1.03±0.07	1.11±0.07
Feed 11	1.28±0.06	1.12±0.06	1.31±0.06	1.23±0.06	1.41±0.06	1.39±0.06	1.45±0.06	1.5±0.06
Feed 12	1.15±0.06	0.94±0.07	1.25±0.06	1.27±0.06	1.43±0.06	1.35±0.06	1.45±0.06	1.6±0.06
Feed 13	1.28±0.06	0.99±0.07	1.29±0.07	1.12±0.07	1.17±0.06	1.09±0.06	1.26±0.05	1.3±0.06
Feed 14	0.97±0.08	0.89±0.08	1.04±0.08	1.03±0.07	1.1±0.07	1.08±0.07	1.16±0.07	1.14±0.07
Feed 15	1.34±0.07	1.29±0.06	1.46±0.07	1.4±0.08	1.44±0.08	1.47±0.08	1.37±0.07	1.31±0.08
Feed 16	1.08±0.07	1.45±0.06	1.34±0.07	1.27±0.06	1.26±0.06	1.25±0.07	1.27±0.06	1.28±0.06
Feed 17	1.11±0.06	1.06±0.07	1.2±0.06	1.31±0.07	1.31±0.06	1.33±0.05	1.37±0.06	1.47±0.06
Feed 18	1.18±0.08	1.19±0.06	1.19±0.07	1.47±0.07	1.35±0.07	1.28±0.07	1.3±0.07	1.46±0.07
Feed 19	0.8±0.07	0.8±0.08	0.91±0.07	0.94±0.07	0.94±0.07	1.02±0.07	0.99±0.07	1.06±0.08